

# Evaluation of three-dimensional cole-cole parameters from spectral IP data

Jeong-Seok Yang<sup>1</sup>, Hee Joon Kim<sup>2</sup>

<sup>1</sup>Seoul National University, Seoul, Korea, <sup>2</sup>Pukyong National University, Busan, Korea

**Abstract:** Clay minerals show a distinct induced-polarization phenomenon, which is one of the most important factors for predicting groundwater flow and contaminant transport. This paper presents a step-by-step process to estimate Cole-Cole parameters from spectral induced-polarization (IP) data measured on the surface of three-dimensional earth. First, the inversion of low-frequency resistivity survey data is made to identify the dc resistivity  $\rho_{dc}$  of a volume having IP effects. The other parameters, chargeability  $m$ , time constant  $\tau$ , and frequency dependence  $c$ , are sought for the polarizable volume. Next, using multi-frequency data,  $c$  can be obtained as high or low asymptotes of the slope of log phase vs. log frequency. Further, for low  $m$ , intrinsic  $\tau$  is approximated by apparent one,  $\tau_a$ , which is derived from the relation  $\omega\tau_a = 1$  at an angular frequency  $\omega$ , where the imaginary component of spectral IP data has an extreme value. Finally, to obtain intrinsic  $m$  a two-step linearized procedure has been derived. For a body of given  $\tau$  and  $c$ , forward modeling with a progression of  $m$  values yields a plot of observed vs. intrinsic imaginary components for a frequency. Since this plot is essentially linear, to extract the intrinsic imaginary component is quite simple with an observed value. Using the plot of intrinsic imaginary component vs.  $m$ , intrinsic  $m$  is determined. We present a synthetic example to illustrate that the Cole-Cole parameters can be recovered from spectral IP data.

## Introduction

Mapping the distribution, fractional amount of type of clay is important in understanding groundwater flow and contaminant transport (Kelly, 1976; Borner et al., 1993). Clay minerals have distinct surface electrical properties and large surface area that lead to decreased electrical resistivity in soils containing them and to a distinctive frequency dependent complex resistivity known as induced polarization (IP). IP depends on the clay type, concentration, cation exchange capacity and other factors, which are nearly the same as those controlling fluid and contaminant transport (Hohmann, 1990). Extraction of intrinsic clay properties from surface surveys would be valuable in all hydrological studies.

IP data have been routinely collected in mineral exploration fields. Excellent reviews on the IP method and case histories can be found in Fink et al. (1990) and Ward (1990). Pelton et al. (1978) proposed the following four-parameter Cole-Cole model to represent the behavior of complex resistivity:

$$\rho(\omega) = \rho_{dc} \left[ 1 - m \left( 1 - \frac{1}{1 + (i\omega\tau)^c} \right) \right], \quad (1)$$

where  $\rho_{dc}$  is the dc resistivity,  $m$  the chargeability,  $\omega$  the angular frequency,  $\tau$  the time constant, and  $c$  the frequency dependence bounded between 0 and 1. Olhoeft (1985) performed a frequency domain analysis for the IP parameters with multi-frequency data. Yuval and Oldenburg (1997) developed a process to estimate Cole-Cole parameters from time-domain IP surveys. Their procedure was to invert individual time channel data separately to obtain a complete decay curve in each cell of parameterized model, and carried out parametric inversion in each cell to recover  $m$ ,  $\tau$ , and  $c$ . Routh and Oldenburg (1998) presented that the spectral parameters in Cole-Cole model could be recovered from multi-frequency complex resistivity data, and performed two-dimensional (2-D) inversion based on a Gauss-Newton approach with regularization. Yang (2002) suggested that 3-D complex resistivity modeling is necessary to simulate IP phenomena for conductive and polarizable objects. Li and Oldenburg (2000) presented an inversion algorithm for evaluating  $m$  in a 3-D environment.

Although most workers used 2-D interpretation, we try to attempt 3-D analysis for deriving the intrinsic IP parameters in the Cole-Cole formulation. We begin our discussion why IP interpretation requires full 3-D modeling (Yang, 2002). In this study a horizontal 3-D slab is used to represent a clay body. We then illustrate our methodology to derive Cole-Cole parameters step by step from spectral IP data under the tabular body assumption and within the detection depth.

## Basic assumptions

Laboratory studies have suggested that the frequency dependence  $c$  is in the range of 0.1 to 0.6 (Madden and Cantwell, 1967) with a mean value near 0.25 (Pelton et al., 1978). Vacquier (1957) and Bodmer et al. (1968) noted pure clay has little polarizability. However, clay-bearing zone (clay-sand mixture) has usually significant polarizability, and it can be found around a pure clay zone with IP methods. Fraser et al. (1964) and Klein et al. (1982) showed the chargeability of clay-bearing sandstone ranges from 0.05 to 0.25. In an aquifer system, since a clay or clay-bearing zone usually exists in a layered shape, a flat 3-D polarizable body can be a good candidate for the initial model in forward modeling.

In this study 3-D complex resistivity analysis is performed for Cole-Cole parameter estimation with the following assumptions:

- 1) Clay or clay-bearing zone is conductive and polarizable so that it has a significant IP effect.
- 2) A horizontal 3-D rectangular slab is used for representing the clay-bearing zone.
- 3) The frequency dependency  $c$  is in the range of 0.1 to 0.6.
- 4) The chargeability has low to moderate value ( $m < 0.5$ ).

The main task of this paper is to determine whether the intrinsic IP parameters of Cole-Cole representation (1) can be recovered from the measured or apparent responses of a multi-frequency surface IP survey. To this end we use a synthetic example to illustrate the process for deriving each Cole-Cole parameter. Since this procedure does not use nonlinear optimization (or inversion scheme) to evaluate  $m$ ,  $\tau$ , and  $c$ , there is no non-uniqueness problem.

## Cole-cole parameter estimation

We develop a process to estimate Cole-Cole parameters from multi-frequency complex resistivity data collected on the surface of 3-D earth. The recovery of the parameters basically takes four steps.

In the first stage, low-frequency apparent resistivity data are inverted to recover the resistivity distribution in the subsurface. The parameter  $\rho_{dc}$  in Cole-Cole equation (1) can thus be derived from the inversion of low-frequency data.

3-D dc resistivity inversion has been relatively well studied by many researchers (Park and Van, 1991; Ellis and Oldenburg, 1994; Sasaki, 1994). Sasaki (1994) made an effective inversion scheme, which employs 3-D forward modeling with a finite-element method (FEM), calculation of sensitivity matrix based on the adjoint-equation approach and a linearized least-squares method with a smoothness constraint. The inversion scheme used in this study is basically same as that of Sasaki (1994) except that an optimum value of Lagrange multiplier is sought at each iteration to find a reasonable balance between data fitting and smoothness constraint.

Figure 1 shows a test model, which consists of a conductive horizontal 3-D slab of  $10 \Omega\text{-m}$  in a uniform  $100 \Omega\text{-m}$  half-space, to check our inversion algorithm. The electrode configuration used is surface dipole-dipole array. The slab is located at the depth  $a$  and its dimension is  $3a \times 4a \times a$ , where  $a$  is the dipole length. The number of survey lines is 9, the interval between two adjacent lines is  $a$ , and each line has 16 electrodes in  $x$ -direction. The FEM mesh has  $80 \times 52 \times 40$  (= 166400) nodes and  $a$  is equivalent to four-node intervals. Inversion is performed with  $15 \times 8 \times 6$  (= 720) blocks in  $x$ -,  $y$ -, and  $z$ -directions and the block dimension is  $a \times a \times a$  except the blocks along the perimeter of inversion zone.

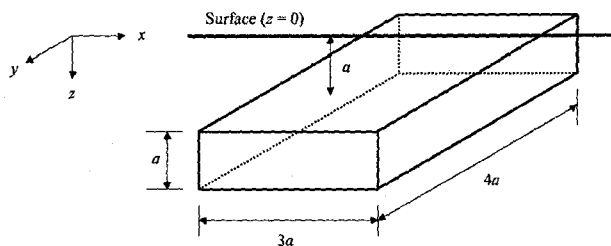


Figure 1. A 3-D model for Cole-Cole parameter inversion.  $\rho_{back} = 100 \Omega\text{-m}$ ,  $\rho_{body} = 10 \Omega\text{-m}$ ,  $m_{body} = 0.3$ ,  $\tau_{body} = 0.1 \text{ sec}$ ,  $c_{body} = 0.25$ , where subscripts *back* and *body* denote the background and body, respectively, and  $a$  is the unit dipole-length.

Prior to the inversion 3 % Gaussian noise is added to the synthetic data derived from the model in Figure 1. The inversion is started with an initial model of 100  $\Omega$ -m homogeneous half-space. Figure 2 shows the inversion result of  $x$ - $z$  resistivity section ( $y = 0$ ). The inversion process is quite stable and after 4 iterations the conductive body is correctly imaged as shown in Figure 2. The conductive body is imaged correctly but it does not achieve amplitude as high as that of the true body and its boundary is smoothed. Once a low resistivity zone is found, we focus our interest on the low-resistivity zone, define the zone as a homogeneous polarizable body, and find out the other Cole-Cole parameters of the body.

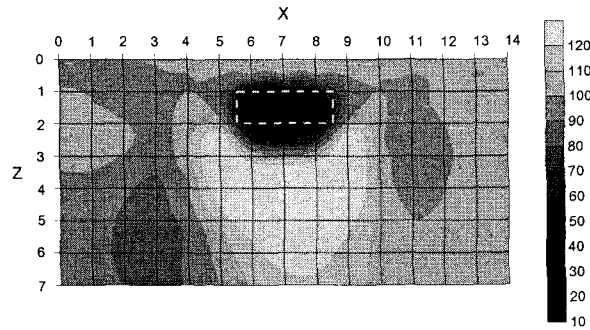


Figure 2. Resistivity section along the profile of  $y = 0$  (center line over the body) derived from the inversion of synthetic data.

The frequency dependence  $c$  may be obtained from a log phase vs. log frequency plot which can be made from multi-frequency IP data; the slope of the phase asymptotes at the very high or very low frequency to show an intrinsic value of  $c$ . To verify this fact we do 2-D complex resistivity modeling at frequencies ranging from  $10^{-6}$  to  $10^6$  Hz. Although this frequency range is practically too wide,  $c$  can be exactly shown at very high and low frequencies. The depth to the top of the body is  $a$ , the width in  $x$  direction is  $3a$ , and the thickness is  $a$ . The polarizability of the body is  $\rho_{dc} = 10.0 \Omega$ -m,  $m = 0.3$ ,  $\tau = 0.1$  sec, and  $c = 0.25$ . The background is non-polarizable 100  $\Omega$ -m half-space. Figure 3 shows a log phase of apparent complex resistivity vs. log frequency plot for a source-receiver pair: (-3, -2) for the source electrodes and (3, 4) for the receiver electrodes. From Figure 3 we can find the slope at the low or high frequency is very close to 0.25, which agrees with the given  $c$  in the 2-D modeling. This indicates  $c$  can be obtained from multi-frequency field data. We can also have  $c$  information for a polarizable 3-D body by phase survey at very low or high frequencies.

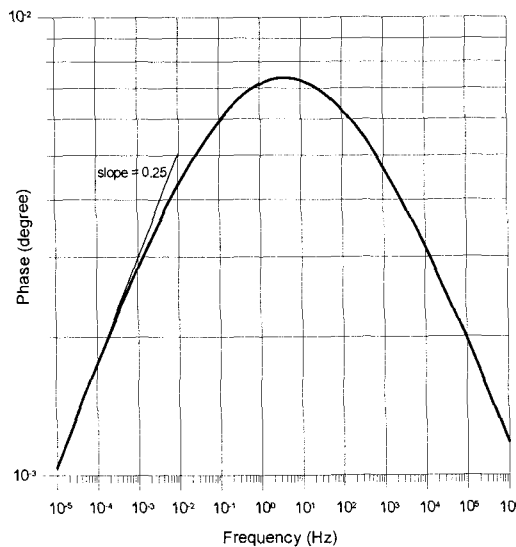


Figure 3. Apparent phase curve as a function of frequency modeled for 2-D polarizable body. The geometry of the body is the same as the 3-D model in Figure 1 in  $x$  and  $z$  direction.  $\rho_{back} = 100 \Omega$ -m,  $\rho_{body} = 10 \Omega$ -m,  $m_{body} = 0.3$ ,  $\tau_{body} = 0.1$  sec,  $c_{body} = 0.25$ .

Although  $c$  can be estimated directly from multi-frequency IP data as described above, we assume it 0.25 after Pelton et al. (1978) in the following discussion. The chargeability  $m$  of clay is known to be rather small (Fraser et al., 1964 and Klein et al., 1982), and this has made it difficult to perform a successful IP survey in the past because instrument accuracy was inadequate (or insufficient). We assume  $m$  is not high ( $m < 0.5$ ).

The apparent time constant  $\tau_a$  can be also determined from multi-frequency IP data. We can pick a frequency at which the imaginary component of apparent complex resistivity has an extreme value for a source-receiver pair. To obtain the frequency we differentiate the imaginary component of Cole-Cole equation (1) with respect to frequency and set it to zero. Then we have the relationship,  $\omega\tau_a = 1$ , and using the relationship and multi-frequency IP data,  $\tau_a$  is obtained.

From multi-frequency complex resistivity modelings, Yang (2002) showed that  $\tau_a$  is almost the same as the intrinsic  $\tau$  when  $m$  is relatively small. Figure 4 shows  $\tau_a$  is very similar to intrinsic  $\tau$  ( $= 1/2\pi$  or 0.159) when the  $m$  is 0.1, 0.2, and 0.3. The  $\tau_a$  in the figure was obtained by using the following steps. First, forward modelings for selected frequencies were performed to have the maximum absolute value of imaginary component for a source-receiver pair. Second, pick the extreme value and the corresponding frequency. Finally, using the relationship ( $\omega\tau_a = 1$ ), calculate the  $\tau_a$  ( $= 1/2\pi f$ ).

If we assume small  $m$  ( $< 0.5$ ), we are able to just pick one dominant  $\tau_a$  value in the pseudo-section and regard it as the intrinsic  $\tau$ . We might have to consider some 'dilution' effect of time constant over the pseudo-section in the decision.

$\tau$  can be estimated from the multi-frequency data by picking a dominant  $\tau_a$  value from the  $\tau$  pseudo-sections like Figure 4 with the low  $m$  assumption. The only unknown parameter is thus the intrinsic  $m$  of the object in this stage.

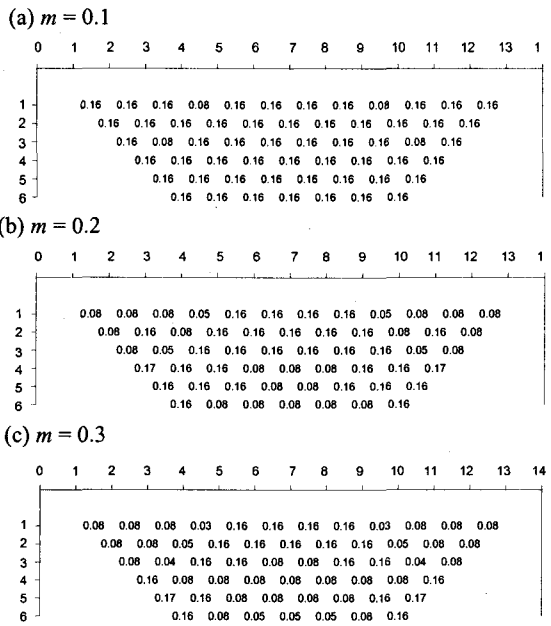


Figure 4. Apparent time constant pseudo-section ( $m = 0.1, 0.2, \text{ and } 0.3, \tau_{body} = 1/2\pi (= 0.159)$ , from Yang (2002)).

### Chargeability estimation

Since the three parameters,  $\rho_{dc}$ ,  $c$ , and  $\tau$ , can be estimated by using the methods described above, we have to determine one remaining parameter,  $m$ , from multi-frequency data. In the following, a final step is suggested to find out  $m$  of a 3-D body. The information of the three parameters and complex resistivity data are necessary for the  $m$  estimation.

To estimate  $m$  two plots are necessary; One is a graph of imaginary components of intrinsic complex resistivities as a function of frequency for different  $m$  (Figure 5). The other is the relationship between imaginary components of intrinsic and apparent complex resistivities (Figure 8). We use the Cole-Cole equation (1) to draw Figure 5 for  $\rho_{dc} = 10 \Omega\text{-m}$  and  $\tau = 0.1 \text{ sec}$ .

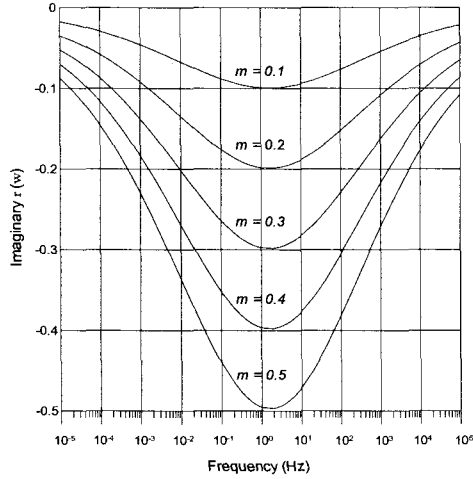
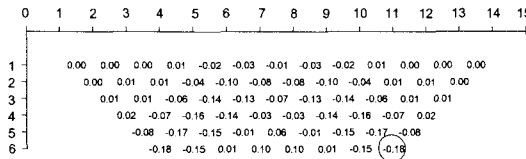


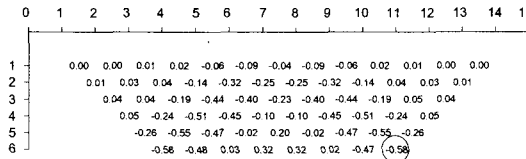
Figure 5. Imaginary components of complex resistivities derived from the Cole-Cole equation for  $\rho_{dc} = 10 \Omega\text{-m}$ ,  $\tau = 0.1 \text{ sec}$ , and  $c = 0.25$ .

The other plot needs several 3-D complex resistivity forward modelings. Since the geometry,  $\rho_{dc}$ ,  $c$ , and  $\tau$  of the body are known, we just change  $m$  to perform the forward modeling. After the forward modelings are performed, we choose one source-receiver pair, which can be considered to represent the IP response from the body, or we can just pick maximum (absolute) imaginary component for a source-receiver pair in each pseudo-section. Figure 6 shows the pseudo-sections from the forward modeling with small  $m$  ( $= 0.1, 0.3, \text{ and } 0.5$ ). The eighth transmitter and sixth receiver pair is selected to choose the imaginary component. The number at the bottom-right corner in the pseudo-section is the imaginary component value for the pair and its absolute value is the maximum one in the pseudo-section for this case.

(a)  $m = 0.1$



(b)  $m = 0.3$



(c)  $m = 0.5$

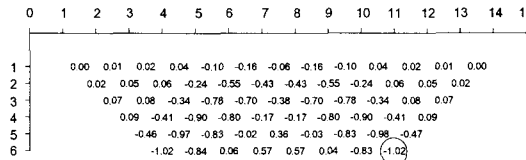


Figure 6. Imaginary component pseudo-section ( $m = 0.1, 0.3, \text{ and } 0.5$ ,  $\tau = 0.1 \text{ sec}$ ,  $f = 1.0 \text{ Hz}$ ).

The relationship between the imaginary components of the intrinsic and apparent complex resistivity can be

established by plotting the imaginary components. We have the imaginary components of intrinsic and apparent complex resistivity for a certain value of chargeability. The intrinsic components were calculated using the Cole-Cole equation and the apparent components were computed from the 3-D complex resistivity forward modeling. We know the chargeability values for the both components. If we pick one chargeability value used in the forward modeling in the previous step, we have the corresponding intrinsic and apparent imaginary components to the chargeability. We picked three values of chargeability so we have three pairs of the intrinsic and apparent imaginary components. The three pairs can be plotted in an intrinsic vs. apparent value plane and Figure 7 shows the relationship is practically linear.

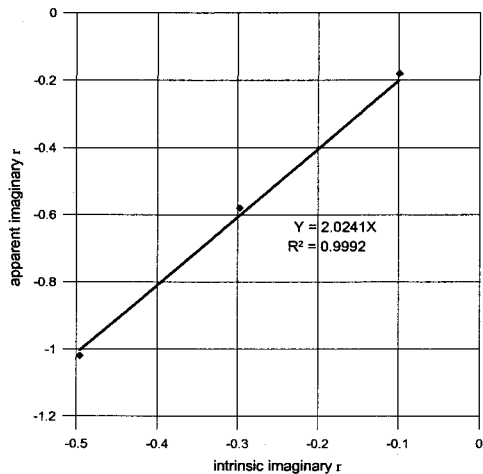


Figure 7. Apparent vs. Intrinsic imaginary component ( $\tau = 0.1$  sec,  $f = 1.0$  Hz).

The final step to estimate the chargeability is to obtain apparent complex resistivity from a body with unknown chargeability. The source-receiver pair in the previous step is selected from data and the imaginary component of the apparent resistivity for the source-receiver pair is checked. We can have the imaginary component of the intrinsic complex resistivity by using the relationship in Figure 7, and then use the relationship between imaginary component of intrinsic complex resistivity and chargeability, like Figure 5, to estimate the chargeability from the imaginary part of the intrinsic complex resistivity. This approximate inversion procedure is robust and works very well for targets of low chargeability. For such targets, we have seen that the intrinsic time constant is approximately the same as the maximum observed time constant. The frequency dependence is unchanged in the observations. The resistivities themselves are well determined from the standard non-linear inversion. It this appears from this research that the intrinsic Cole-Cole parameters can be deduced from field data, at least for the case of isolated clay bodies.

### Conclusions

We have developed a process to estimate Cole-Cole parameters from spectral IP data measured on the surface of 3-D earth. The evaluation of parameters takes four steps. First, the inversion of low-frequency resistivity survey data is made to identify  $\rho_{dc}$  of a volume having IP effects. The other parameters,  $m$ ,  $\tau$ , and  $c$ , are sought for the polarizable volume. Next, using multi-frequency data,  $c$  can be obtained as high or low asymptotes of the slope of log phase vs. log frequency. Further, for low  $m$ , intrinsic  $\tau$  is approximated by apparent one,  $\tau_a$ , which is derived from the relation  $\omega\tau_a = 1$  at an angular frequency  $\omega$ , where the imaginary component of spectral IP data has an extreme value. Finally, to obtain intrinsic  $m$  a two-step linearized procedure has been derived. For a body of given  $\tau$  and  $c$ , forward modeling with a progression of  $m$  values yields a plot of observed vs. intrinsic imaginary components for a frequency. Since this plot is essentially linear, to extract the intrinsic imaginary component is quite simple with an observed value. Using the plot of intrinsic imaginary component vs.  $m$ , intrinsic  $m$  is determined.

The field measurement of broadband complex resistivity data and the analysis with them can be the future study of this research.

## References

- Bodmer, R., S. W. Ward, and H. F. Morrison, 1968. On induced polarization and groundwater. *Geophysics*, v. 33, pp. 805-821.
- Borner, F. D., J. R. Schopper, and A. Weller, 1996. Evaluation of transport and storage properties in the soil and groundwater zone from induced polarization measurements. *Geophys. Prosp.*, v. 44, pp. 583-601.
- Ellis, R. G., and D. W. Oldenburg, 1994. The pole-dipole 3-D DC resistivity inverse problem: a conjugate-gradient approach. *Geophys. J. Int.*, v. 119, pp. 187-194.
- Fink, J. B., McAlister, E. O., Sternberg, B. K., Widuwilt, W. G., and Ward, S. H., Eds., 1990. *Induced Polarization: Applications and Case Histories*, Soc. Expl. Geophys.
- Fraser, D. C., N. B., Jr. Keevil, and S. H. Ward, 1964. Conductivity spectra of rocks from the Craigmont ore environment. *Geophysics*, v. 29, pp. 832-847.
- Hohmann, G. W., 1990, Three-dimensional IP models, *in* Fink, J. B. et al., Eds., *Induced Polarization: Applications and Case Histories*, Soc. Expl. Geophys., pp. 150-178.
- Iliceto, V., G. Santarato, and S. Veronese, 1982. An approach to the identification of fine sediments by induced polarization laboratory measurements. *Geophys. Prosp.*, v. 30, pp. 331-347.
- Kelly, W. E., 1976. Geoelectric sounding for delineating groundwater contamination. *Ground Water*, v. 14, pp. 6-10.
- Klein, J. D., and W. R. Sill, 1982. Electrical properties of artificial clay-bearing sandstone. *Geophysics*, v. 47, pp. 1593-1605.
- Li, Y., and Oldenburg, D. W., 2000. 3-D inversion of induced polarization data. *Geophysics*, v. 65, pp. 1931-1945.
- Madden, T. R., and T. Cantwell, 1967. Induced polarization, a review, *in* *Mining Geophysics*, Vol. 2, Soc. Expl. Geophys., pp. 373-400.
- Olhoeft, G. R., 1985. Low-frequency electrical properties. *Geophysics*, v. 50, pp. 2492-2503.
- Park, S. K., and G. P. Van, 1991, Inversion of pole-pole data for 3-D resistivity structure beneath arrays of electrodes, *Geophysics*, v. 56, pp. 951-960.
- Pelton, W. H., S. H. Ward, P. G. Hallof, W. R. Sill, and P. H. Nelson, 1978. Mineral discrimination and removal of inductive coupling with multifrequency IP. *Geophysics*, v. 43, pp. 588-609.
- Routh, P. S., D. W. Oldenburg, and Y. Li, 1998. Regularized inversion of spectral IP parameters from complex resistivity data. 68th Ann. Int. Mtg., Soc. Expl. Geophys., Expanded Abstracts, pp. 810-813.
- Sasaki, Y., 1994. 3-D resistivity inversion using the finite-element method. *Geophysics*, v. 59, pp. 1839-1848.
- Vacquier, V., C. R. Holmes, P. R. Kintzinger, and M. Lavergne, 1957, Prospecting for ground water by induced electrical polarization. *Geophysics*, v. 22, pp. 660-687.
- Ward, S. H., 1990, Resistivity and induced polarization method, *in* Ward, S. H., Ed., *Geotechnical and Environmental Geophysics*, Soc. Expl., Geophys., pp. 147-190.
- Yang, J.-S., 2002. Three-dimensional complex resistivity analysis for clay characterization in hydrogeologic study. Ph.D. Thesis, Univ. of California at Berkeley.
- Yuval, and D. W. Oldenburg, 1997. Computation of Cole-Cole parameters from IP data. *Geophysics*, v. 62, pp. 436-448.